

## Electrochemically synthesized Pt/TiO<sub>2</sub>-C catalysts for direct methanol fuel cell applications

Alexandra B. Kuriganova,<sup>\*a</sup> Igor N. Leontyev,<sup>b</sup> Alexander S. Alexandrin,<sup>a</sup>  
Olga A. Maslova,<sup>b,c,d</sup> Aydar I. Rakhmatullin<sup>e</sup> and Nina V. Smirnova<sup>a</sup>

<sup>a</sup> Department of Technology, M. I. Platov South-Russian State Polytechnic University, 346428 Novocherkassk, Russian Federation. E-mail: kuriganova\_@mail.ru

<sup>b</sup> Department of Physics, Southern Federal University, 344006 Rostov-on-Don, Russian Federation

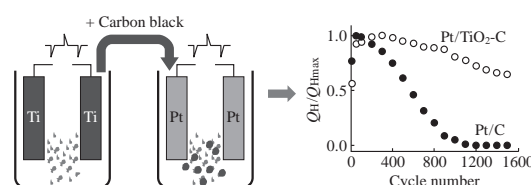
<sup>c</sup> Universidade Federal de Minas Gerais, 31270-010 Belo Horizonte, Brazil

<sup>d</sup> Tomsk State University, 634050 Tomsk, Russian Federation

<sup>e</sup> Universite d'Orleans, 45067 Orleans, France

DOI: 10.1016/j.mencom.2017.01.021

The Pt/TiO<sub>2</sub>-C catalysts with different TiO<sub>2</sub> loadings have been prepared by electrochemical oxidation/dispersion, and their good catalytic activity in CO stripping and methanol electrooxidation reactions has been shown.



The electrocatalytic activity and degradation stability of electrocatalysts based on Pt nanoparticles (NPs) determines the performance of proton-exchange membrane fuel cells (PEMFCs). Electrochemically active surface area (ECSA) losses in the catalyst due to carbon support oxidative corrosion<sup>1</sup> and the subsequent agglomeration of Pt NPs cause catalyst degradation.

In this context, metal oxides (MO<sub>x</sub>) are promising supports for Pt NPs. However, the low electronic conductivity of the MO<sub>x</sub> does not allow for the complete elimination of carbon from the catalytic system. Therefore, the electronic conductivity and corrosion stability of a hybrid MO<sub>x</sub>-C support have to be balanced during the operation of PEMFCs.<sup>2</sup>

Various MO<sub>x</sub> are used as oxide components in Pt-based catalysts.<sup>3</sup> The application of TiO<sub>2</sub> as a support for Pt catalysts is due to its availability and the strongest interaction between the surfaces of Pt NPs and TiO<sub>2</sub>.<sup>4</sup> This significantly decreases the agglomeration of Pt nanoparticles upon fuel cell operation. The Pt-TiO<sub>2</sub> nanostructures are usually synthesized *via* the sequential reduction of Ti and Pt precursor concentrations.<sup>5</sup> However, the electrochemical synthesis of TiO<sub>2</sub> and Pt nanostructures was not widely used.<sup>6–8</sup>

In this work, we studied the electrochemical properties of TiO<sub>2</sub>-C-supported Pt NPs, which served as anode catalysts in a methanol oxidation reaction (MOR). Previously, we applied this technique to the synthesis of MO<sub>x</sub><sup>9–11</sup> and Pt-containing catalysts<sup>9–11</sup> based on different carbon<sup>7,12,13</sup> and metal oxide supports.<sup>14,15</sup>

Nanosized TiO<sub>2</sub> was prepared by the electrochemical oxidation and dispersion of Ti electrodes.<sup>11</sup> The Pt/TiO<sub>2</sub>-C catalysts

were obtained analogously to Pt/C catalysts<sup>†</sup> as described elsewhere.<sup>7</sup> The platinum loading in the catalysts was 25±0.5%, and the amounts of TiO<sub>2</sub> were 10, 30 and 60%.

Figure 1 shows the X-ray powder diffraction (XRD) patterns<sup>‡</sup> of freshly prepared Pt/TiO<sub>2</sub>-C catalysts, Pt/C and TiO<sub>2</sub> synthesized under similar conditions. The XRD pattern of Pt/TiO<sub>2</sub>-C has diffraction peaks attributed to the face centered cubic (fcc) structure of Pt and titanium dioxide as anatase and rutile. However, the concentration of anatase in the Pt/TiO<sub>2</sub>-C nanocomposite was much higher than that of rutile. According to the XRD data, the average Pt and TiO<sub>2</sub> crystallite sizes evaluated from the Scherrer equation were 10.6 and 10.3 nm, respectively.

The TEM images of the samples (Figure 2)<sup>§</sup> reveal the uniform distribution of Pt particles over the carbon black and the MO<sub>x</sub>

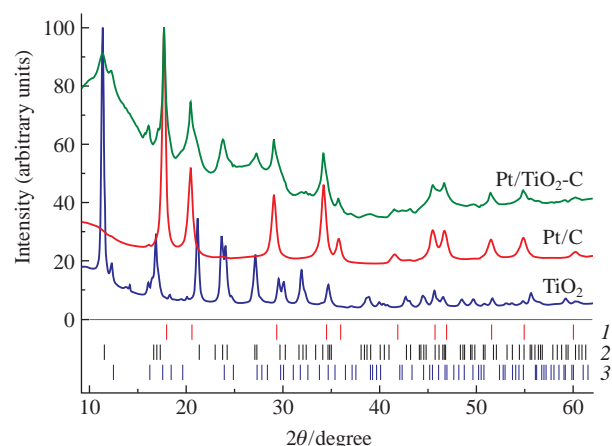


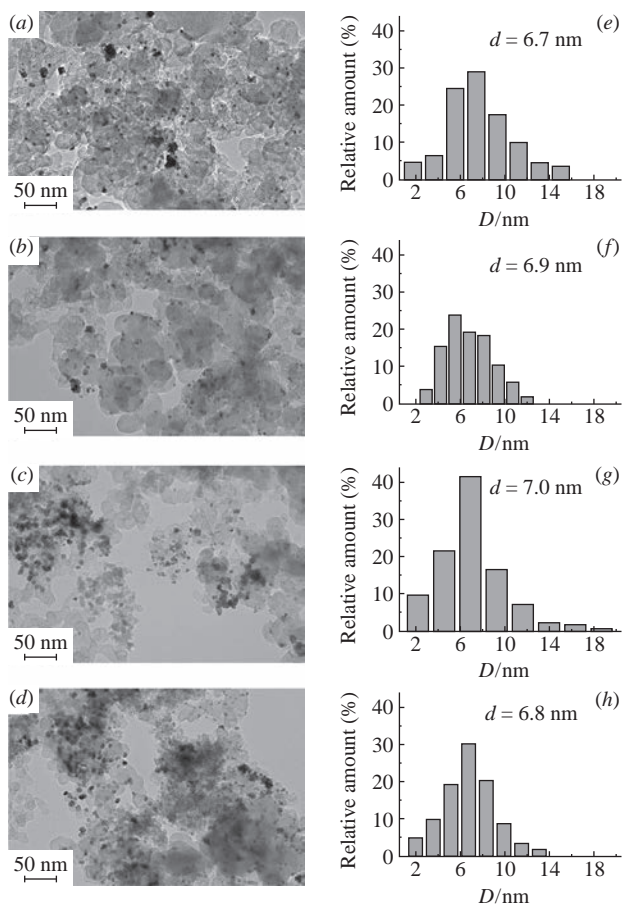
**Figure 1** XRD patterns of TiO<sub>2</sub> powders, Pt/C and Pt/TiO<sub>2</sub>-C catalysts (30% TiO<sub>2</sub>). The tick marks correspond to fcc structures of (1) Pt, (2) anatase and (3) rutile phases in TiO<sub>2</sub>.

<sup>†</sup> For the preparation of Pt/TiO<sub>2</sub>-C catalysts, TiO<sub>2</sub> powder was mixed with Vulcan XC-72 carbon black (Cabot Corp., 240 m<sup>2</sup> g<sup>-1</sup>) in an aqueous 2 M NaOH solution. Two Pt electrodes with the same areas were immersed in the suspension and connected to an ac source (50 Hz). In turn, the platinum electrodes were dispersed by the applied alternating current with symmetrical pulses, as described above. The suspension was then filtered, and the catalysts were rinsed with H<sub>2</sub>O to neutral pH and dried at 80 °C to constant weight.

<sup>‡</sup> X-ray measurements were carried out at the Swiss–Norwegian beam lines of the European Synchrotron radiation facility at the radiation wavelength λ = 0.694724 Å using a 2-D Pilatus2M detector (Dectris).

**Table 1** Electrochemical characteristics of Pt/C and Pt/TiO<sub>2</sub>-C catalysts.

Catalyst	TiO <sub>2</sub> content (%)	CO stripping			Methanol electrochemical oxidation			
		$E_{\text{onset}}/\text{mV}$	$E_{\text{peak}}/\text{mV}$	$\text{ECSA}/\text{m}^2 \text{g}_{\text{Pt}}^{-1}$	$E_{\text{peak}}/\text{mV}$	$j_{\text{peak}}/\text{mA cm}_{\text{Pt}}^{-2}$	$j_{600\text{mV}}/\text{mA cm}_{\text{Pt}}^{-2}$	$I_f/I_b$
Pt/C	–	670	800	10.8	835	0.43	0.087	1.70
Pt/TiO <sub>2</sub> -C	10	540	700	11.6	866	1.07	0.120	0.84
	30	600	730	5.7	866	1.01	0.223	0.81
	60	550	700	8.3	863	0.93	0.147	0.78

**Figure 2** (a)–(d) TEM images and (e)–(h) particle size distributions in (a), (e) Pt/C and Pt/TiO<sub>2</sub>-C catalysts: (b), (f) 10% TiO<sub>2</sub>, (c), (g) 30% TiO<sub>2</sub> and (d), (h) 60% TiO<sub>2</sub>.

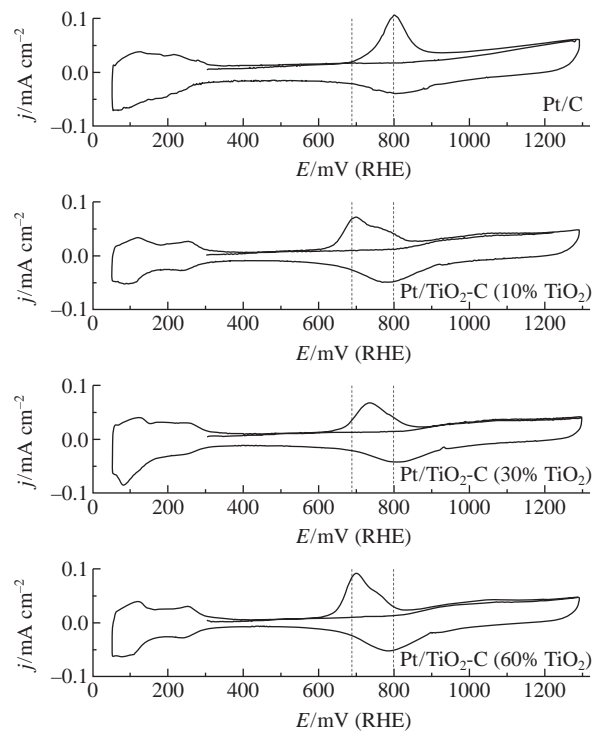
structure composed of individual grains with a small amount of aggregates especially typical of the Pt/TiO<sub>2</sub>-C sample with 30% TiO<sub>2</sub>. The average surface Pt particle sizes estimated from the TEM data were 6.7 and 6.8–7.0 nm for Pt/C and Pt/TiO<sub>2</sub>-C catalysts, respectively. Thus, TiO<sub>2</sub> in the catalytic system exerts no influence on the Pt nanoparticle size distribution; this is consistent with published data.<sup>16</sup>

The electrochemical characterization of Pt-based catalysts was described previously.<sup>14</sup> The ECSA of Pt/C and Pt/TiO<sub>2</sub>-C catalysts was prepared *via* CO stripping.<sup>17</sup> The CV curves (Figure 3) of Pt/TiO<sub>2</sub>-C catalysts compared to those of Pt/C catalyst after the CO adsorption contain the electrooxidation peaks of CO<sub>ads</sub> species in a potential range of 600–900 mV, which is typical of Pt. The presence of 10% TiO<sub>2</sub> or more in the electrocatalyst causes a decrease in the onset potential and in the CO oxidation peak at potential of 70–100 mV compared

to Pt/C catalyst (Table 1). A similar effect was observed in the Pt/SnO<sub>x</sub>-C catalytic system.<sup>14,16</sup> Note that the highest overvoltage of CO oxidation on the Pt/TiO<sub>2</sub>-C catalytic system occurred on Pt/TiO<sub>2</sub>-C (30% TiO<sub>2</sub>). The minimum ECSA was also found in the Pt/TiO<sub>2</sub>-C (30% TiO<sub>2</sub>) catalyst. This can be due to the irregular distribution of Pt particles on the TiO<sub>2</sub>-C support. This fact is in agreement with the TEM image of Pt/TiO<sub>2</sub>-C (30% TiO<sub>2</sub>) [Figure 2(c)].

An increased TiO<sub>2</sub> loading in Pt-based catalysts caused no further decrease in the CO electrooxidation overvoltage on the Pt surface; this is consistent with published data.<sup>16</sup>

A similar effect during the electrochemical oxidation of methanol on the synthesis of catalysts was also observed. Figure 4(a) shows the MOR curves attributed to Pt/TiO<sub>2</sub>-C and Pt/C catalysts. An increase in the methanol oxidation rate by a factor of 2–5 for Pt/TiO<sub>2</sub>-C catalysts with various TiO<sub>2</sub> loadings as compared with the Pt/C catalyst was revealed. The mechanism of methanol electrooxidation in the presence of a metal oxide component can be explained in the context of the bifunctional catalysis theory.<sup>18</sup> The adsorption of oxygen-containing species at the MO<sub>x</sub> surface in acid electrolytes is known to occur on the cathodic potentials rather than on platinum. Therefore, the lower the adsorption potential of the oxygenated species, the lower the oxidation potential of adsorbed organic species. The ratio between the current density of the anodic peaks in the forward scan ( $I_f$ ) and the back scan ( $I_b$ ) decreases with raising the TiO<sub>2</sub> loading in Pt-based catalysts (Table 1). The  $I_f/I_b$  parameter is related to

**Figure 3** CO stripping on Pt/C and Pt/TiO<sub>2</sub>-C catalysts; scan rate, 20 mV s<sup>-1</sup>; CO was adsorbed at  $E = 300$  mV vs. RHE.

§ The particle size distribution was studied by transmission electron microscopy (TEM) on a Hitachi HT-7700 TEM system (High-Technologies Europe GmbH) at a field emission of 100 kV.

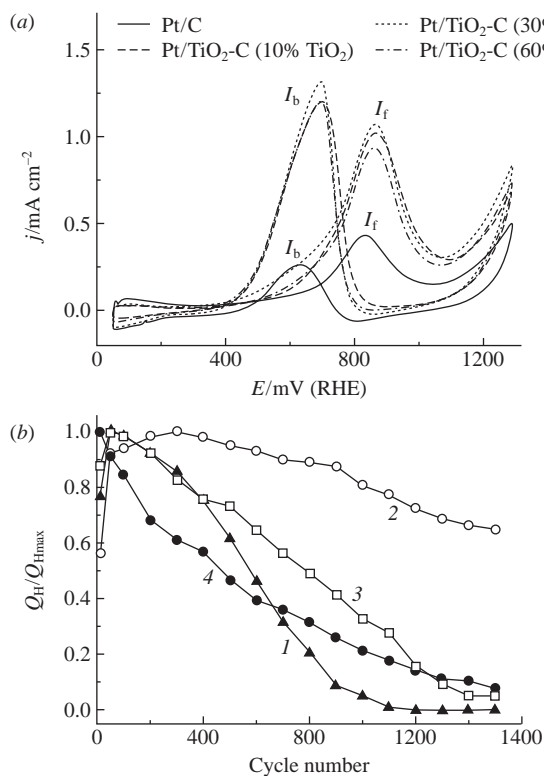


**Figure 4** (a) CV curves of Pt/C and Pt/TiO<sub>2</sub>-C catalysts in a 0.5 M MeOH + 0.5 M H<sub>2</sub>SO<sub>4</sub> solution acquired at a scan rate of 50 mV s<sup>-1</sup>; and (b) normalized  $Q_H$  during cycling in 0.5 M H<sub>2</sub>SO<sub>4</sub> at a scan rate of 50 mV s<sup>-1</sup>: (1) Pt/C, (2) Pt/TiO<sub>2</sub>-C (10% TiO<sub>2</sub>), (3) Pt/TiO<sub>2</sub>-C (30% TiO<sub>2</sub>), and (4) Pt/TiO<sub>2</sub>-C (60% TiO<sub>2</sub>).

the degree of coverage with oxygenated species.<sup>19</sup> This fact is consistent with a MOR rate in Pt/TiO<sub>2</sub>-C catalysts superior to that of Pt/C catalyst [Figure 4(a)].

Figure 4(b) shows that the high stability of the Pt/TiO<sub>2</sub>-C (10% TiO<sub>2</sub>) electrocatalyst, determined by an accelerated stress test,<sup>†</sup> can be attributed to a strong metal–support interaction between Pt particles and the TiO<sub>2</sub> support.<sup>20</sup> We assume that the low stability of Pt/TiO<sub>2</sub>-C catalysts with 30 and 60% TiO<sub>2</sub> is due to the low conductivity of hybrid supports at high TiO<sub>2</sub> contents.

Thus, we found that the presence of TiO<sub>2</sub> in Pt-based catalysts obtained *via* electrochemical oxidation/dispersion increased with the electrocatalytic activity of Pt-based catalysts during methanol oxidation by a factor of 2–5, which was attributed to the gaining

degree of coverage with oxygenated species at lower potentials onto the Pt/TiO<sub>2</sub>-C catalyst surface as compared to Pt/C catalyst. The Pt/TiO<sub>2</sub>-C catalysts with 10% TiO<sub>2</sub> exhibited the highest stability due to an optimal ratio between the electronic conductivity of the MO<sub>x</sub>-C support and the support component loading.

This work was supported by the Russian Science Foundation (grant no. 14-23-00078).

## References

- I. N. Leontyev, D. V. Leontyeva, A. B. Kuriganova, Yu. V. Popov, O. A. Maslova, N. V. Glebova, A. A. Nechitailov, N. K. Zelenina, A. A. Tomasov, L. Hennem and N. V. Smirnova, *Mendelev Commun.*, 2015, **25**, 468.
- A. B. Kuriganova, D. V. Leontyeva, S. Ivanov, A. Bund and N. V. Smirnova, *J. Appl. Electrochem.*, 2016, **46**, 1245.
- N. R. Elezovic, V. R. Radmilovic and N. V. Krstajic, *RSC Adv.*, 2016, **6**, 6788.
- A. S. Zyubin, T. S. Zyubina, Yu. A. Dobrovolskii, A. A. Bel'mesov and V. M. Volokhov, *Russ. J. Inorg. Chem.*, 2014, **59**, 816 (*Zh. Neorg. Khim.*, 2014, **59**, 1038).
- S. Shanmugam and A. Gedanken, *Small*, 2007, **3**, 1189.
- A. Jaroenworarluck, D. Regonini, C. R. Bowen, R. Stevens and D. Allsopp, *J. Mater. Sci.*, 2007, **42**, 6729.
- I. Leontyev, A. Kuriganova, Y. Kudryavtsev, B. Dkhil and N. Smirnova, *Appl. Catal., A*, 2012, **431–432**, 120.
- O. A. Petrii, *Russ. Chem. Rev.*, 2015, **84**, 159.
- D. V. Leontyeva, I. N. Leontyev, M. V. Avramenko, Yu. I. Yuzyuk, Yu. A. Kukushkina and N. V. Smirnova, *Electrochim. Acta*, 2013, **114**, 356.
- A. B. Kuriganova, C. A. Vlaic, S. Ivanov, D. V. Leontyeva, A. Bund and N. V. Smirnova, *J. Appl. Electrochem.*, 2016, **46**, 527.
- A. Kuriganova, A. Alexandrin and N. Smirnova, *Key Eng. Mater.*, 2016, **683**, 419.
- N. V. Smirnova, A. B. Kuriganova, D. V. Leont'eva, I. N. Leont'ev and A. S. Mikheikin, *Kinet. Catal.*, 2013, **54**, 255 (*Kinet. Katal.*, 2013, **54**, 265).
- N. V. Smirnova, A. B. Kuriganova, K. S. Novikova and E. V. Gerasimova, *Russ. J. Electrochem.*, 2014, **50**, 899 (*Elektrokhimiya*, 2015, **50**, 999).
- A. B. Kuriganova and N. V. Smirnova, *Mendelev Commun.*, 2014, **24**, 351.
- D. E. Doronkin, A. B. Kuriganova, I. N. Leontyev, S. Baier, H. Lichtenberg, N. V. Smirnova and J.-D. Grunwaldt, *Catal. Lett.*, 2016, **146**, 452.
- H. Song, X. Qiu, F. Li, W. Zhu and L. Chen, *Electrochem. Commun.*, 2007, **9**, 1416.
- M. J. Watt-Smith, J. M. Friedrich, S. P. Rigby, T. R. Ralph and F. C. Walsh, *J. Phys. D: Appl. Phys.*, 2008, **41**, 174004.
- T. Iwashita, *Electrochim. Acta*, 2002, **47**, 3663.
- D. Y. Chung, K.-J. Lee and Y.-E. Sung, *J. Phys. Chem. C*, 2016, **120**, 9028.
- S.-Y. Huang, P. Ganesan, S. Park and B. N. Popov, *J. Am. Chem. Soc.*, 2009, **131**, 13898.

<sup>†</sup> The durability and the stability of electrocatalysts were compared by cycling the work electrode in a potential range of 50–1300 mV (RHE) in a 0.5 M H<sub>2</sub>SO<sub>4</sub> solution at a scan rate of 50 mV s<sup>-1</sup>.

Received: 8th August 2016; Com. 16/5020